[65]In early experiments by T. M. Buck (private communication), a similar sample (but with a Ga end contact) gave the sublinear range, while one from a nearby region of the same crystal did not.

[66]H. C. Casey, Jr. and F. Ermanis (unpublished).

[67]Though well suited for the junction case of Sec. II D2, the independent variable W would be less convenient here than F.

[68]By considering $d\bar{M}/d\gamma$ along the hyperbola short of the minimum-conductivity point, $\gamma<0$ can be shown to hold for p type, and $\gamma>0$ for n type.

PHYSICAL REVIEW B VOLUME 5, NUMBER 6 15 MARCH 1972

Valence-Band Structure of $PtSb_2$

D. H. Damon,* R. C. Miller, and P. R. Emtage
Westinghouse Research Laboratories, Pittsburgh, Pennsylvania 15235
(Received 28 June 1971)

The low-temperature galvanomagnetic properties of p-type $PtSb_2$ are reported for magnetic fields up to 60 kG, using samples with extrinsic current-carrier densities from 6×10^{16} to 1.5×10^{19} cm^{-3}. From the low-field properties and the Shubnikov–de Haas oscillations it is found that the valence-band maxima are six ellipsoids on ⟨100⟩ axes, the principal inertial effective masses being in the ratio 0.61 : 1 : 1.64, the least cyclotron mass $(0.168\pm0.005)m$, and scattering close to isotropic. The band parameters are found to be independent of the energy of the current carrier, suggesting a direct band gap greater than 0.4 eV; cf. indirect band gap of about 0.1 eV. The ratio of effective masses was obtained by analyzing small beats in the amplitude of the oscillations in the resistivity.

I. INTRODUCTION

In this paper we report the valence-band structure of platinum antimonide $PtSb_2$, a narrow-band-gap semiconductor of the pyrite structure. A number of inquiries into the preparation, transport properties, optical properties, and band structure of this material have been published.[1–6] Here we give measurements of the magnetoresistance and Hall coefficient of p-type $PtSb_2$ at low temperatures 1.3–4.2 °K, in magnetic fields up to 60 kG, for samples with extrinsic carrier concentrations between 6×10^{16} and 1.5×10^{19} cm^{-3}.

From prior work[2] we know the valence-band maxima of $PtSb_2$ to be centered on the ⟨100⟩ axes. The pyrite structure is of cubic class T_h, invariant under twofold rather than fourfold rotations about the principal axes. From the point of view of this paper the most interesting consequence of this symmetry is that a band maximum on one of the principal axes, at $[k00]$ say, is characterized by three *unequal* principal effective masses (m_1, m_2, m_3). Masses at the equivalent stationary points are obtained by a cyclic permutation of the indices; e.g., at $[0\pm k\,0]$ the effective masses are (m_3, m_1, m_2). One result of this symmetry is that when a current flows in the [100] direction the transverse magnetoresistances with $H\parallel[010]$ and with $H\parallel[001]$ need not be the same, and generally are not.

The band gap of $PtSb_2$ is small, about 0.10 eV,[2,3] so it would not be surprising to find that the effective masses are dependent on the Fermi level. A calculation by one of the authors[6] suggests that the warping of the bands may be unusually large in this material. Our investigation was therefore carried out over the wide range of carrier concentrations noted above; no sign of a dependence of any of the effective masses on the energy of the holes was found.

Section III is rather long and involved. We briefly outline this discussion so as to indicate clearly which results we believe to be the most important and what conclusions may be drawn from them. We first examined that part of the low-field magnetoresistance that is quadratic in the field strength. From the data one can find the ratio $m_1/\tau_1 : m_2/\tau_2 : m_3/\tau_3$, m_i and τ_i being principal effective masses and relaxation times. The results provide a test of the multivalley model and preliminary values of the effective-mass ratios if the relaxation time is presumed isotropic. The interpretation of these results is made difficult by the presence of a negative magnetoresistance in most of the samples. At high fields Shubnikov–de Haas oscillations are observed in both the magnetoresistance and the Hall coefficient. We obtain the periods and amplitudes of these oscillations as a function of carrier concentration, temperature, and orientation of the magnetic field. Each period is inversely proportional to a stationary area of the Fermi surface measured normal to the direction of the field; for a general field direction the six valence-band maxima have three distinct stationary areas. The observed oscillations are due to the smallest of these areas, since oscillations due to the greater areas are more strongly damped by

scattering. The existence of weaker oscillations with shorter periods results in interference effects; these effects are quite marked in $PtSb_2$ because the valence-band maxima are not very far from being spherical, so oscillations due to the greater areas are not very much less in size than those due to the principal area. The interference effects are not strong enough to insert extra zeros into the oscillations.

An accurate determination of the angular dependence of the periods is sufficient to give the geometry of the Fermi surface. We are unable to find the periods well enough to obtain accurate values of the effective-mass ratios since we can resolve, at best, three complete oscillations, and even these few are made irregular by interference effects. The results, however, do verify that the shape of the Fermi surface does not depend on the number of current carriers.

The temperature dependence of the amplitude at fixed field is, as usual, used to determine the cyclotron masses. After making allowance for interference effects it is found that these masses are independent of the carrier concentration, and that their angular variation matches the angular variation of the areas. It is concluded that the energy of a current carrier is quadratic in its wave number.

The field dependence of the amplitudes extrapolated to absolute zero is the only part of our high-field results that enables us to improve on the ratios of inertial effective masses that were estimated from the low-field magnetoresistance. When only one period is present, $H \parallel [111]$ for ellipsoids centered on the $\langle 100 \rangle$ axes, the amplitude is exponentially dependent on H^{-1}, a preexponential factor $H^{1/2}$ being easily allowed for. When two or more periods are present interference effects result in deviations from this rule. These deviations are clearly visible in our measured amplitudes and can be fitted to an ellipsoidal model of the band structure by adjusting the ratios of the principal inertial effective masses.

II. EXPERIMENTAL PROCEDURE AND RESULTS

Conventional dc techniques were used to measure the galvanomagnetic coefficients. The sample current was supplied by a North Hills CS-12 current source. The magnet was a Westinghouse superconducting solenoid with a maximum field of about 60 kG. Current contacts were soldered to the bar-shaped specimens. The voltage probes were pressed point contacts of Be-Cu held in place by springs of Be-Cu or silver solder. In the usual way, four voltage probes were used so that two values each of the resistivity and Hall coefficient were measured on each sample.

To facilitate the accumulation of the large amount of data required to study the Shubnikov–de Haas oscillations we employed an automated data-acquisition system. Figure 1 is a schematic diagram of this apparatus. The programmer, consisting of stepping switches and time-delay circuits, first switched on a motor which drove a potentiometer to increase the magnet current for a preset time. Simultaneously the programmer switched the digital voltmeter into an integrating mode which measured the change in the magnetic field strength as the time integral of the voltage induced in a small coil placed near the sample. Next the programmer switched the digital voltmeter into a voltmeter mode and selected voltages which the voltmeter measured. Sequentially the sample current, the galvanomagnetic voltages for both directions of current, a zero voltage (measured with the voltmeter terminals shorted in order to check the adjustment of the voltmeter), and the magnet current were measured. The programmer then switched to the position where the magnetic field was again increased by a small amount and the above procedure was repeated until the highest possible field strength was reached. The magnet current was then reduced to zero, the magnet-current direction reversed, and the same measurements made for this field direction. All the measurements reported here were made with the samples immersed in liquid helium under a controlled vapor pressure. Thus, we could be sure that a complete run, that might take as long as 3 h, was made at a temperature constant to $\pm 0.01\,^{\circ}K$.

The measured voltages were recorded on paper tape using Hewlett-Packard model Nos. 2545 A tape punch coupler and 2545C paper tape handler. The tapes were read into the Westinghouse Research Laboratory computer which reduced the measured voltages to magnetoresistance ratios and Hall coefficients. The procedure for obtaining values of

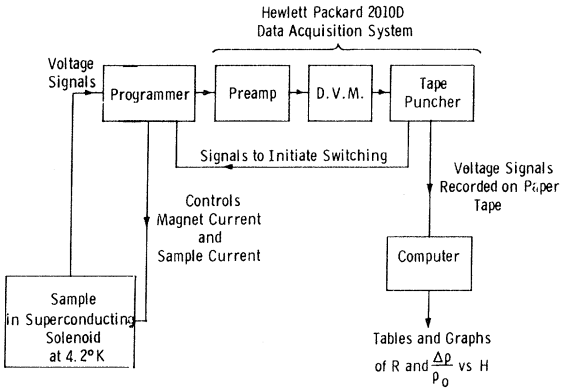

FIG. 1. Schematic flow diagram of the apparatus. A stepping switch in the "programmer" controls the magnetic field strength and the accumulation of the galvanomagnetic voltages.

the magnetic field strength was as follows. A magnetic field strength in the neighborhood of 30 kG was calculated from one measured value of the magnet current using the calibration constant supplied by the manufacturer. All other field strengths were calculated from this point using the measured integrated flux. This procedure gives field strengths accurate within 100 G. Between 10 and 60 kG the fractional error is less than 1%. At low fields (below 5 kG) one sees the error in a spurious field dependence of the Hall coefficient. Since the galvanomagnetic voltages were not measured at exactly the same field strengths for the two directions of field it was necessary to interpolate all measured voltages to values appropriate to a preselected set of equally spaced field values. At these fields the usual averages over both directions of field and current were then taken to calculate the magnetoresistance ratio $\delta\rho/\rho_0$ and the Hall coefficient R. These results were obtained in the form of tables and graphs as a function of field strength.

The samples were cut in the form of rectangular parallelepipeds about $10\times2\times1$ mm from Czochralski ingots. The preparation and characterization of our material has been described elsewhere.[1]

Table I lists values of the Hall coefficients and resistivities of the samples used in this investigation. Ir and Rh substituted for Pt and Sn substituted for Sb act as acceptors in $PtSb_2$. As is indicated in the table most of the sample used in this investigation were Rh doped. Where comparisons can be made the mobilities are in good agreement with most of the results reported by others.[3-5] We draw attention to two of the samples. Sample 1, like all samples with low carrier concentration, shows a mobility at 4.2 °K that is much less than that at 77 °K; no oscillations were observed in such samples. Sample 5b is much the same as 5a, being cut from a neighboring site in the ingot with its length along another of the ⟨100⟩ axes; this sample was prepared so as to check the apparently anomalous effective mass obtained from 5a, and confirmed it.

Longitudinal and transverse magnetoresistance ratios for fields in the [100] direction are exhibited in Fig. 2, for sample 1 of low carrier concentration and mobility, and in Fig. 3 for several samples of higher carrier concentration and mobility in which Shubnikov–de Haas oscillations can be observed. Individual points are omitted because they are only 0.4 kG apart and the scatter is too small to be shown on these figures. For comparison, note that the longitudinal [100] magnetoresistance is zero in degenerate samples at 77 °K, and the transverse magnetoresistance is positive and proportional to H^2 at low fields; this behavior is expected for ellipsoidal bands on the principal axes. By contrast, the low-temperature results in Fig. 2 show initial negative and later positive magnetoresistances in both longitudinal and transverse directions. The positive and negative components are markedly temperature dependent; we have not investigated the effects shown at these low carrier concentrations.

At higher carrier concentrations, Fig. 3, the non-oscillatory part of the longitudinal magnetoresistance is always negative; it will be seen that sample 2, $R = 13$ cm^3/C, apparently belongs in the low concentration regime if one judges by the exceptional behavior of its longitudinal magnetoresistance. The non-oscillatory part of the transverse magnetoresistance in the other samples appears to be a sum of the longitudinal magnetoresistance and a normal positive component that is virtually independent of temperature.

Oscillatory components of the magnetoresistance and Hall coefficient are shown in Figs. 4 and 5, after the smooth variation has been subtracted out. Figure 4 shows points on the [100] longitudinal oscillations at three temperatures for sample 4a, $R = 1.9$ cm^3/C. In fairness, we should note that these points are unusually regular; there is generally a discernible scatter in the neighborhood of the max-

TABLE I. Characteristics of p-type $PtSb_2$ samples; the low-field Hall coefficient R (cm^3/C), resistivity ρ (Ω cm), and Hall mobility μ_H (cm^2/V sec), at 77 and 4.2 °K.

Sample number	Dopant	Current direction	77 °K R	77 °K ρ	77 °K μ_H	4.2 °K R	4.2 °K ρ	4.2 °K μ_H
1	?	[001]	98	4.1×10^{-2}	2450	150	0.169	890
2	Sn	[100]	14.5	6.3×10^{-3}	2460	13.0	6.4×10^{-3}	2030
3	Rh	[100]	8.1	4.0×10^{-3}	2030	7.87	3.05×10^{-3}	2600
4a	Rh	[100]	2.0	1.18×10^{-3}	1700	1.87	9.14×10^{-4}	2050
4b	Rh	[110]	1.96	1.16×10^{-3}	1700	1.84	9.3×10^{-4}	1980
5a	Rh	[100]	1.26	8.0×10^{-4}	1580	1.17	6.4×10^{-4}	1830
5b	Rh	[010]	1.18	7.76×10^{-4}	1520	1.11	6.0×10^{-4}	1850
5c	Rh	[0$\bar{1}$1]		not measured		1.13	6.25×10^{-4}	1810
5d	Rh	[001]		not measured		1.19	6.32×10^{-4}	1880
6	Rh	[100]	0.426	3.6×10^{-4}	1180	0.422	3.3×10^{-4}	1300

ima.

We shall remark here on a couple of points that are not clearly related to the band structure and will not be mentioned in Sec. III. The negative term in the longitudinal magnetoresistance is greatest at low concentrations and temperatures; as Roth *et al.*[7] observed, it appears to exist primarily at concentrations near to or somewhat greater than those at which an impurity band is formed. The functional dependence at fields above 5 kG can be represented by $\Delta\rho/\rho_0 = A - \alpha H^n$, in which A is small and almost independent of temperature, and α decreases while n increases with increase in temperature; for sample 3, $R \sim 8$ cm^3/C, we find $n \simeq 0.36 + T/60$.

In Fig. 5 oscillations in the Hall coefficient are shown that are roughly the same size as those in the transverse magnetoresistance and nearly out of phase with them. Variations in the diagonal components of σ alone produce variations in $R = \sigma_{xy}/H(\sigma_{xx}\sigma_{yy} + \sigma_{xy}^2)$ that are in phase with those in $\rho = \sigma_{xx}/(\sigma_{xx}\sigma_{yy} + \sigma_{xy}^2)$ provided that $\sigma_{xy}^2 < \sigma_{xx}\sigma_{yy}$, a condition that is satisfied in this case. The behavior of R and ρ implies oscillations in σ_{xy} that are out of phase with those in the diagonal components, and of comparable size. The variations in σ_{xy} are not due to any redistribution of electrons between bands that might result from variations in the relative free energies of different bands, since similar behavior is observed when the field is along a [111] direction and all bands are then equivalent.

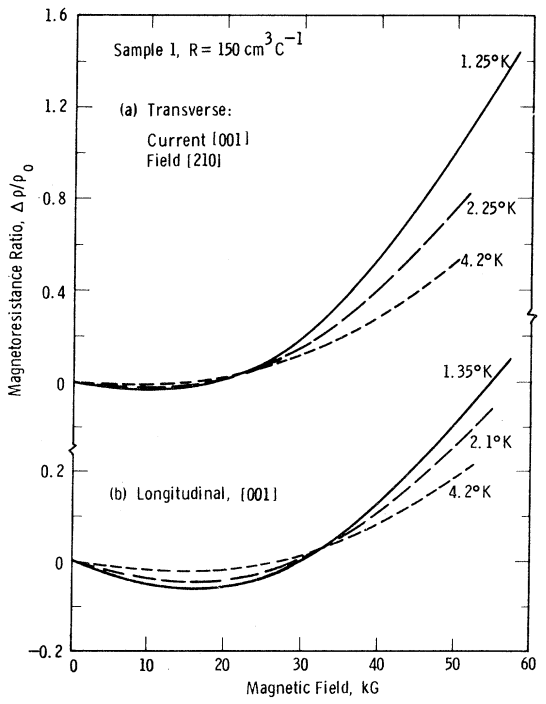

FIG. 2. Transverse and longitudinal magnetoresistance ratios for sample 1, of low carrier concentration and with a small mobility at low temperatures. Note scale changes.

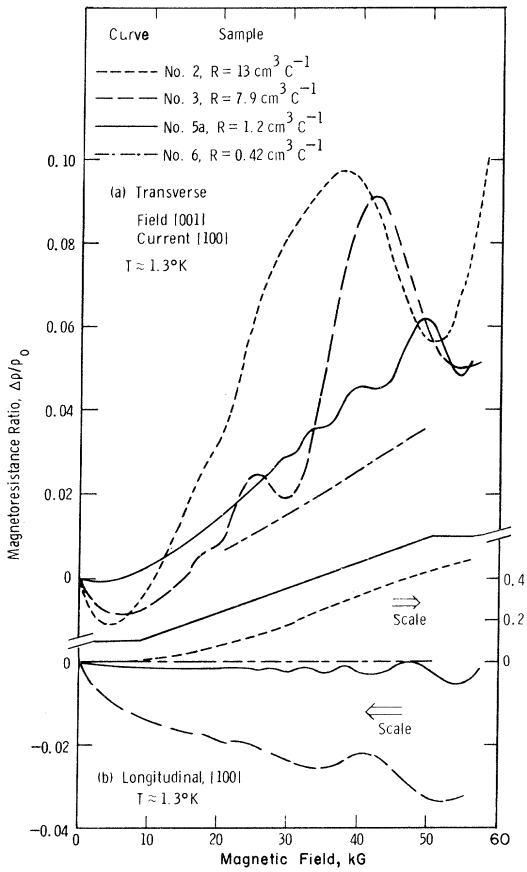

FIG. 3. Transverse and longitudinal magnetoresistance ratios of four samples with moderate-to-high carrier concentration, at low temperature. Note scale for longitudinal magnetoresistance of sample 2.

The non-oscillatory part of the Hall coefficient is only slightly field dependent. In all cases except sample 1 it increases steadily with increase in field; at the highest fields it is 3–7% greater than the low-field value. In sample 1 a similar decrease occurs.

III. DISCUSSION

A. Low Fields

The negative part of the magnetoresistance appears to be independent of both the field and current *directions* for a given carrier concentration and temperature, except in the two samples with lowest carrier concentration; these samples are omitted from the following discussion. Subtraction of the longitudinal magnetoresistance from a transverse resistance taken at the same temperature yields a smoothly varying positive resistance that is quadratic in H for fields below 15 kG and is independent of temperature. This we consider to be

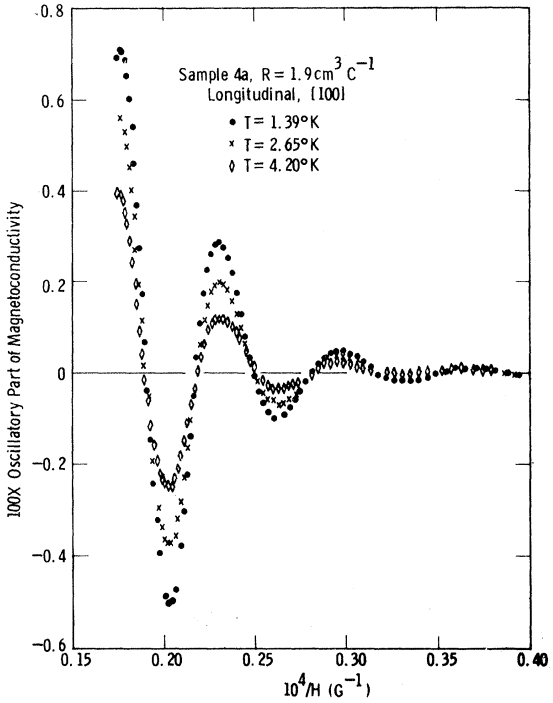

FIG. 4. Oscillatory part of the longitudinal magnetoconductivity ratio of sample 4a at three temperatures, plotted against $10^4/H$; the slowly varying part of the magnetoconductivity has been subtracted out. All high-field points taken at 1.39 °K are shown; some of the points taken at the two higher temperatures are omitted because of overlap. Measurements taken at three other temperatures are omitted altogether.

a normal quadratic term given by the usual expansion in powers of H.

From prior work,[2] the valence bands are ellipsoids centered on the ⟨100⟩ axes, having three unequal principal effective masses m_1, m_2, m_3, and principal relaxation times τ_1, τ_2, τ_3. Assuming degenerate statistics, the galvanomagnetic coefficients of such bands are[8]

$$R = r/nec\ ,$$
$$\frac{\Delta\rho}{\rho_0 H^2} = b + c(l_i\gamma_i)^2 + dl_i^2\gamma_i^2 + e\epsilon_{ijk}l_j^2\gamma_k^2\ , \tag{1}$$

in which ϵ_{ijk} is the unit antisymmetric tensor and the double-suffix summation convention is implied. Here R is the Hall coefficient, n the number of current carriers, $\Delta\rho$ the change in resistivity at magnetic field H, and l_i, γ_i are the direction cosines of the current and magnetic field referred to the crystal axes. The constants b, c, d, e, and r are given in terms of the band structure and Hall mobility μ_H by

$$\frac{b}{\mu_H^2} = -1 + \frac{K_1+K_2+K_1K_2}{2K_1K_2(1+K_1+K_2)^2}$$
$$\times (K_1^2+K_2^2+K_1K_2^2+K_1^2K_2+K_1+K_2)\ ,$$
$$\frac{c}{\mu_H^2} = 1 - \frac{3(K_1+K_2+K_1K_2)}{(1+K_1+K_2)^2}\ ,$$
$$\frac{e}{\mu_H^2} = \frac{(K_1+K_2+K_1K_2)(K_1-K_2)(K_1-1)(K_2-1)}{2K_1K_2(1+K_1+K_2)^2}$$
$$d = -(b+c)\ , \qquad r = 1-c\ , \tag{2}$$

where

$$K_1 = m_3\tau_2/m_2\tau_3\ , \quad K_2 = m_1\tau_2/m_2\tau_1\ .$$

These relationships hold for crystal class T_h, and differ from the better-known relationships[9] for class O_h primarily in the existence of the coefficient e. For class O_h one must have either K_1 or K_2 equal to unity, or $K_1 = K_2$, and the above equations then reduce to more familiar forms.

At low temperatures, samples 3–6 give similar magnetoresistance coefficients b, d, and e, the scatter being 10% about the mean values; the relationship $b+c+d=0$ holds approximately, but c is difficult to obtain accurately since it is smaller than the others. In all of the samples, the coefficients found at 77 °K are smaller than those found at 4.2 °K; even sample 3, which is at best partially degenerate at the higher temperature, shows a diminished value of b. The high-temperature co-

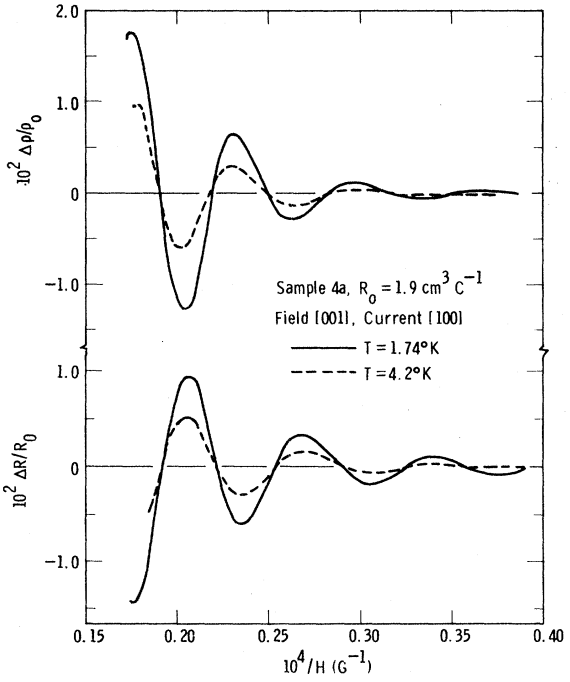

FIG. 5. Oscillatory part of the transverse magnetoresistance and Hall coefficient in sample 4a at two temperatures, plotted against $10^4/H$; the steady part of the variation with field has been removed. No measurements were taken at other temperatures.

efficients found from these samples are 5–10% greater than the best results of our prior work. Our best estimates of the independent coefficients b, c, and e are shown in Table II together with the band parameters K_1 and K_2 and the value of r deduced from them.

These results are anomalous; the relative magnetoresistance $\Delta\rho/\rho_0(\mu_H H)^2$ decreases with increase in temperature even for samples that are only partially degenerate at the higher temperature. Nondegenerate samples do, however, show the expected increase.[10] The effect results from an alteration in the ratios $m_1/\tau_1 : m_2/\tau_2 : m_3/\tau_3$, which change from 0.7 : 1 : 1.6 at the low temperature to 0.7 : 1 : 1.4 at 77 °K. The natural place to look for such an effect is in an alteration in τ_3 relative to τ_1 and τ_2; some straightforward explanations are listed and dismissed below.

(i) The low-temperature scattering is anisotropic. Anisotropic mechanisms can drastically affect the low-temperature magnetoresistance, but only when the mobility is much greater than in these crystals. Moreover, it will be found later that the effective-mass ratios are roughly 0.61 : 1 : 1.64, so the low-temperature relaxation time is the more isotropic of the two.

(ii) Intraband phonon scattering is most likely to be anisotropic for bands that are nearly spherical and not centered on $k = 0$.[11] The observed effect cannot be due to this source of anisotropy since the decreases in mobility that result from the rise in temperature are variously between 10 and 30% for different samples. A fixed degree of anisotropy in the phonon scattering would therefore give a large scatter in the 77 °K results.

(iii) The effect may be altogether hallucinatory, since the low-temperature results involve subtracting away a negative magnetoresistance that is not understood. However, in the sample with the greatest carrier concentration the negative component is zero, while in that with the least carrier concentration the negative component is greater than the quadratic part. These samples give values for b and e that are within 10% of each other, so no essential error can be involved in the subtraction process.

We do not understand the unusual temperature dependence of the magnetoresistance; the low-temperature results give a good preliminary estimate of the effective-mass ratios if τ is presumed isotropic.

TABLE II. Low-field magnetoresistance coefficients b, c, and e at low temperatures and at 77 °K for degenerate samples, and the ratios K_1, K_2, and r found from them.

Temperature (°K)	b/μ_H^2	c/μ_H^2	e/μ_H^2	K_1	K_2	r
≤4.2	0.12	~0.05	0.022	1.6	0.7	0.94
77	0.080	~0.03	0.014	1.4	0.7	0.96

B. High Fields

1. *Introduction*

Many accounts of Shubnikov–de Haas effects have been given; the equations that follow are taken from a review article by Roth and Argyres[12] and hold for the region $\omega_H\tau \gg 1$, ω_H being the cyclotron frequency. At such high fields oscillations in the Hall coefficient are small; the oscillations we observe have been used only to help determine the period P. All our measurements are taken in the region $\omega\tau \lesssim 1$, but the observed variations in the magnetoresistance fit the high-field theory reasonably well and we have used it throughout.

For a simple band the calculated magnetoresistance is of the form

$$\Delta\rho/\rho_0 = R(H) + A(H, T)\cos(2\pi/PH - \tfrac{1}{4}\pi) \qquad (3)$$

in which $R(H)$ is a smoothly varying function, $R(H) = 0$ for the longitudinal magnetoresistance; $A(H, T)$ is the amplitude of oscillations that are of period P in units of G^{-1}. $A(H, T)$ and P are given by

$$P = 2\pi e/\hbar c\, \mathfrak{a}\,, \quad A(H, T) = A_0(H)x/\sinh x\,, \qquad (4)$$

in which

$$x = 2\pi^2 kT/\hbar\omega_H\,, \quad A_0(H) = C(\tfrac{1}{2}HP)^{1/2} e^{-\pi/\omega_H\tau_s}\,,$$

and C is $\frac{5}{2}$ in the transverse case and 1 in the longitudinal case. In these relationships $\mathfrak{a}$ is a stationary area of the Fermi surface, $\mathfrak{a} = \pi k_F^2$ for a spherical surface; τ_s is a relaxation time for scattering, and for anisotropic scattering is expected to be smaller than the momentum relaxation time τ_c that is involved in conduction processes; m_H and ω_H are the cyclotron mass and frequency, respectively,

$$m_H = \frac{\hbar^2}{2\pi}\frac{\partial \mathfrak{a}}{\partial E}\,, \quad \omega_H = \frac{eH}{m_H c}\,.$$

2. *Periods and Cyclotron Masses*

A general characteristic of our results is that only one period P is observed when the field is in any particular direction, but that the amplitudes and intervals between zeros are plagued with irregularities resulting from interference by oscillations of shorter period; the interfering oscillations are smaller in amplitude than the main component since they are more strongly damped by scattering. For example, when the field is in the [110] direction on sample 5d the intervals in $10^5/H$ between consecutive zeros in the magnetoresistance are 0.21, 0.22, 0.24, 0.22, 0.21, 0.19. With the field in the [111] direction on sample 5c, all valleys being

expected to be equivalent in this case, a corresponding set of intervals is 0.17, 0.19, 0.19, 0.19, 0.17, 0.19.

Despite this irregularity the samples as a whole fit together well. Zeros in the magnetoresistance are expected to occur at values of $1/PH = \frac{3}{4}, \frac{5}{4}, \frac{7}{4}, \ldots$, from Eq. (3). Figure 6 shows the positions of the zeros in the longitudinal magnetoresistance for all [100] samples plotted against half integers; results for different samples are close enough for us to be satisfied that only one main period is involved and that interference effects are not drastic. If the argument of the cosine in Eq. (3) is written as $(2\pi/PH - \phi)$, then from Fig. 6 one finds $\phi = (0.2 \pm 0.12)\pi$; the expected value is $\frac{1}{4}\pi$.

Cyclotron masses are found from the temperature dependence of the amplitude at fixed field. This amplitude is expected to obey the relationship

$$\frac{A(H,T)}{T} \sim \frac{1}{\sinh(\alpha H/T)} , \qquad (5)$$

α being proportional to the effective mass; see Eq. (4). Figure 7 shows fits of A/T to the 1/sinh law using effective masses estimated by a system described below. In Fig. 7(b) the field is in a [111] direction for which all valence-band maxima are equivalent; the 1/sinh law is obeyed reasonably well and a single effective mass fits the variation at all of the higher fields; low-field amplitudes are too small to measure accurately. In Fig. 7(a) the field is in a [110] direction for which the various valence-band maxima are inequivalent; interference effects complicate the results, and no single effective mass will fit the variation in amplitude with temperature at all of the higher fields. Note that the effective mass used in drawing the curves of Fig. 7(a) is not the same as that listed below because the highest field amplitudes are shown in the figure; these were discarded in determining the "best" effective mass for reasons mentioned below.

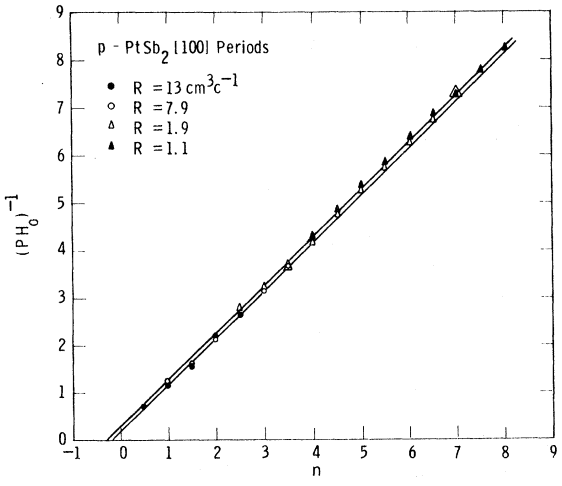

FIG. 6. Values of $1/PH$ at the zeros in the oscillatory part of the [100] longitudinal magnetoresistance plotted against the half-integers, for all [100] samples that exhibit oscillations.

Irregular results such as those of Fig. 7(a) are difficult to analyze graphically since a variety of masses can be chosen as the best fit depending on the criteria used. The following method of determining the cyclotron masses was adopted and used in all cases, regular or irregular, so as to stop preconceptions from leaking in. A series of amplitudes as a function of temperature was found at each of the various magnetic fields at which $\Delta\rho$ was stationary. For fixed H, the run of amplitudes was either retained, given a weight of one-half, or discarded, depending on the apparent accuracy of the measurements; the amplitude of the stationary point observed at the highest field in any run was always discarded because the zero cannot be determined accurately in its neighborhood unless the envelope of the amplitudes is regular, which it generally is not. This weighting was undertaken before finding any effective masses, so as to avoid bias. For a given field the value of α [see Eqs. (4) and (5)] such that the product $(A/T)\sinh(\alpha H/T)$ was most nearly constant was found; there is generally little latitude in the choice. The weighted mean of the series of α's found at different fields was then taken and gave the effective mass. The scatter in each series of α's is generally random in appearance; no systematic variation with field was found. Taking all series of α's into account, the standard error in the mean of a series is found to be 4.2% on average, so the greatest probable error in 8%.

Periods were determined from as many as possible of the magnetoresistances and Hall coefficients for a particular field direction; they are subject to a possible 2–3% error from the irregularities in the position of the zeros. Table III shows the periods P and cyclotron masses m_H found according to the above system; samples with current in the [100] direction have results for all three ⟨100⟩ field directions together and should yield the most accurate results.

The quantity P_{HS} is the period calculated from the Hall coefficient for six equal and spherical valence-band maxima. The ratio P/P_{HS} shown in the fifth column of Table III is independent of carrier concentration if the Fermi surface has the same shape at all energies. P/P_{HS} should then be a function of orientation only, and within experimental error it is; the error includes a possible 2% error in P_{HS} due to errors in the Hall coefficient resulting from uncertainties in sample geometry.

The quantity $m_H P/mP_{HS}$ shown in the sixth column of Table III is independent of both orientation and

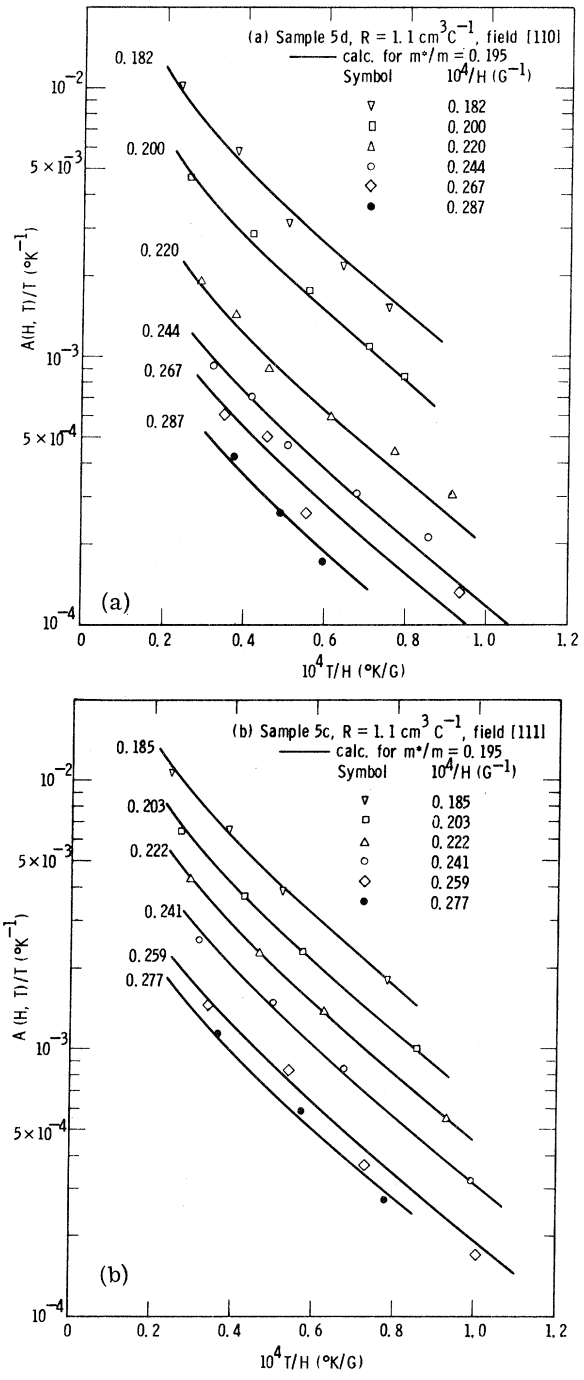

FIG. 7. Temperature dependence of the amplitudes $A(H, T)$ at various fields H for (a) field in the [110] direction and (b) field in the [111] direction. Solid lines are the calculated temperature dependence for the masses shown, with arbitrary positions on the vertical axis.

carrier concentration if the energy is of second order in the wave number, since in this case $P \sim 1/\mathcal{A}$ and $m_H \sim \mathcal{A}/\mathcal{A}_{HS}$. This quantity shows nc systematic drift with carrier concentration, so the bands must be presumed quadratic.

The last two columns of Table III exhibit a correction to the effective masses for the effect of interference by shorter periods. The correction is described at the end of this section; it involves the band structure, the scattering time τ_s, and the details of the way in which the effective mass was calculated. We show it here primarily because there is a very substantial discrepancy between the [100] effective masses obtained from samples 4a and 5a, and we wish to show that this difference (which is greater than the experimental error) is explicable.

The results in Table III are not sufficiently accurate to determine the three principal axes of the constant-energy surfaces (not even ellipsoids of revolution can be ruled out, though unequal axes are expected). This inaccuracy comes from the fact that we can resolve, at best, three complete oscillations, and that even these few are made irregular by interference effects. It will be shown later, from an analysis of interference effects on the amplitude of the oscillations, that the principal inertial effective masses are in the ratio 0.61 : 1 : 1.64. The principal areas are $\mathcal{A}_1 \sim (m_2 m_3)^{1/2}$, etc., and are proportional to the cyclotron effective masses. For magnetic field in the direction $[lmn]$ the stationary area of an ellipsoid with principal areas $\mathcal{A}_1$, $\mathcal{A}_2$, $\mathcal{A}_3$ is given by

$$1/\mathcal{A}^2 = l^2/\mathcal{A}_1^2 + m^2/\mathcal{A}_2^2 + n^2/\mathcal{A}_3^2 .$$

Table IV compares ratios of areas calculated from the principal effective masses with the observed values obtained from Table III, using $P \sim 1/\mathcal{A}$. The observed ratio is in each case sufficiently close to the least calculated ratio; the greater calculated areas do not contribute to the observed period because the oscillations that they cause are more strongly damped by scattering.

The last column of Table IV shows $P_{[100]}/P_{HS}$; the calculated value takes full account of the effective masses and relaxation times, while the observed value is the most accurate such ratio that we have. The discrepancy between the two, though small, is genuine, and we are not able to account for it. Similar disagreements are found in materials with simpler band structures.[13]

3. *Amplitudes*

It has been noted that when more than one period is present the smaller periods, though not resolved, cause erratic variations in the intervals between zeros, the low-temperature amplitudes, and the temperature dependence of the amplitudes. Of these, only the low-temperature amplitudes $A_0(H)$ can be found well enough for conclusions to be drawn about the ratio of the effective masses.

The calculation that follows is intended to give only the direction in which $A_0(H)$ varies with field,

TABLE III. Periods P and effective masses m_H for all samples in which Shubnikov–de Haas oscillations are observed. P_{HS} is the period derived from the Hall coefficient assuming six equivalent and spherical valence-band maxima. Corrected masses allow for interference by periods other than the principal observed period [text Eq. (8)].

			Observed values				Corrected values	
Sample	I	H	$P\times10^5$ (G^{-1})	m_H/m (± 8%)	P/P_{HS}	m_HP/mP_{HS}	m_H/m	m_HP/mP_{HS}
2	[100]	⟨100⟩	2.(6)[a]	0.1(6)[a]	1.(5)[a]	0.2(4)[a]	...	...
3	[100]	⟨100⟩	1.72	0.16_5	1.41	0.23	0.17_5	0.25
4a	[100]	⟨100⟩	0.64	0.18_5	1.36	0.25	0.17_5	0.24
4b	[110]	[1$\bar{1}$0]	0.577	0.18_5	1.24	0.23	0.18	0.22
		[1$\bar{1}$1]	0.540	0.19_5	1.16	0.23	0.19_5	0.23
5a	[100]	⟨100⟩	0.475	0.15_5[b]	1.39	0.22	0.16_5	0.23
5c	[110]	[1$\bar{1}$1]	0.367	0.19_5	1.09_5	0.21	0.19_5	0.21
		[1$\bar{1}$2]	0.40	0.19_5	1.19	0.22	0.19	0.22
5d	[100]	[011]	0.44	0.19	1.27	0.24	0.19	0.24

[a]Very inaccurate; sample shows single poorly-resolved oscillation. [b]Confirmed by sample 5b, similar to 5a.

not its absolute magnitude. Three bands with periods P_1, P_2, P_3($P_1>P_2$, P_3) give an oscillatory magnetoresistance that is approximately of the form

$$\left(\frac{\Delta\rho}{\rho_0}\right)_{T=0}\simeq C(\tfrac{1}{2}HP_1)^{1/2}\left[e^{-\gamma_1/H}\cos\left(\frac{2\pi}{P_1H}\right)+e^{-\gamma_2/H}\cos\left(\frac{2\pi}{P_2H}\right)+e^{-\gamma_3/H}\cos\left(\frac{2\pi}{P_3H}\right)\right], \quad (6)$$

in which

$$C=\begin{cases}\frac{5}{6}, & \text{transverse},\\ \frac{1}{3}, & \text{longitudinal},\end{cases} \qquad \gamma_i=\frac{\pi m_i c}{e\tau_s},$$

and the phase factor $\frac{1}{4}\pi$ has been dropped for clarity. It has been assumed that the bands are of not very different conductivities and periods, and so contribute equally to the oscillations in the absence of damping.

The magnitude of the oscillations is dominated by the term $e^{-\gamma_1/H}$ that multiplies the principal period P_1. Analysis is simplified if one multiplies the amplitudes by the expected exponential variation,

$$A_0(H)\left(\frac{2}{HP_1}\right)^{1/2}e^{\gamma_1/H}$$
$$=\text{envelope of } C\left[\cos\left(\frac{2\pi}{P_1H}\right)+e^{-(\gamma_2-\gamma_1)/H}\cos\left(\frac{2\pi}{P_2H}\right)+e^{-(\gamma_3-\gamma_1)/H}\cos\left(\frac{2\pi}{P_3H}\right)\right], \quad (7)$$

$\gamma_i=\mathfrak{A}_i\gamma_{[100]}/\mathfrak{A}_{[100]}$.

Such analysis depends on finding one of the damping constants γ, others being obtained from it through Eq. (7) with the aid of the calculated ratios of areas in Table IV. In this material, all periods P are the same when H is in a [111] direction, so a logarithmic plot of $A_0/H^{1/2}$ vs H^{-1} yields a straight line of slope $\gamma_{[111]}$ for this orientation of the field.

In finding $A_0(H)$ from the measured amplitudes $A(H, T)$ we eliminated the higher-temperature amplitudes because effects due to greater areas are more strongly reduced by temperature. Two or three of the lowest-temperature amplitudes $A(H, T)$ (or one only on two temperature runs) were extrapolated back to $T=0$ using the $x/\sinh x$ temperature dependence given in Eq. (4); the effective mass used in the extrapolation was the observed value reported in Table III. This is a small extrapolation, the observed amplitudes being increased only by 10–30%, so we expect the effect of greater areas to be well represented.

As is expected from Eq. (6), it was found that a logarithmic plot of $A_0(H)/H^{1/2}$ vs H^{-1} was not usually a straight line, except when H is in a [111] direction. The prescription of Eq. (7) was therefore followed. $A_0(H)$ was multiplied by the expected exponent obtained from the slope of the [111] plot, and the results are shown in Fig. 8 compared with the calculated envelopes. Calculated values are not expected to do better than follow the trends of the observed values, and they do this reasonably well except in the case of sample 5a—bottom right of the figure—which is commented on later. The effective-mass ratio used is the result of a rather tedious attempt to fit the experimental amplitudes to Eq. (7).

TABLE IV. Ratios of observed cyclotron masses and areas, compared with those calculated for $m_1:m_2:m_3=0.61:1:1.64$. The last column is $\mathfrak{A}_{HS}/\mathfrak{A}_{[100]}=P_{[100]}/P_{HS}$.

		[100]	[110]	[111]	[211]	HS
obs	m/m_{100}	1.0	1.11	1.16	1.1	
	$\mathfrak{A}/\mathfrak{A}_{100}$	1.0	1.11	1.23	1.17	1.39
calc		1.0	1.12	1.23	1.10	1.33
		1.28, 1.64	1.21, 1.43		1.25, 1.39	

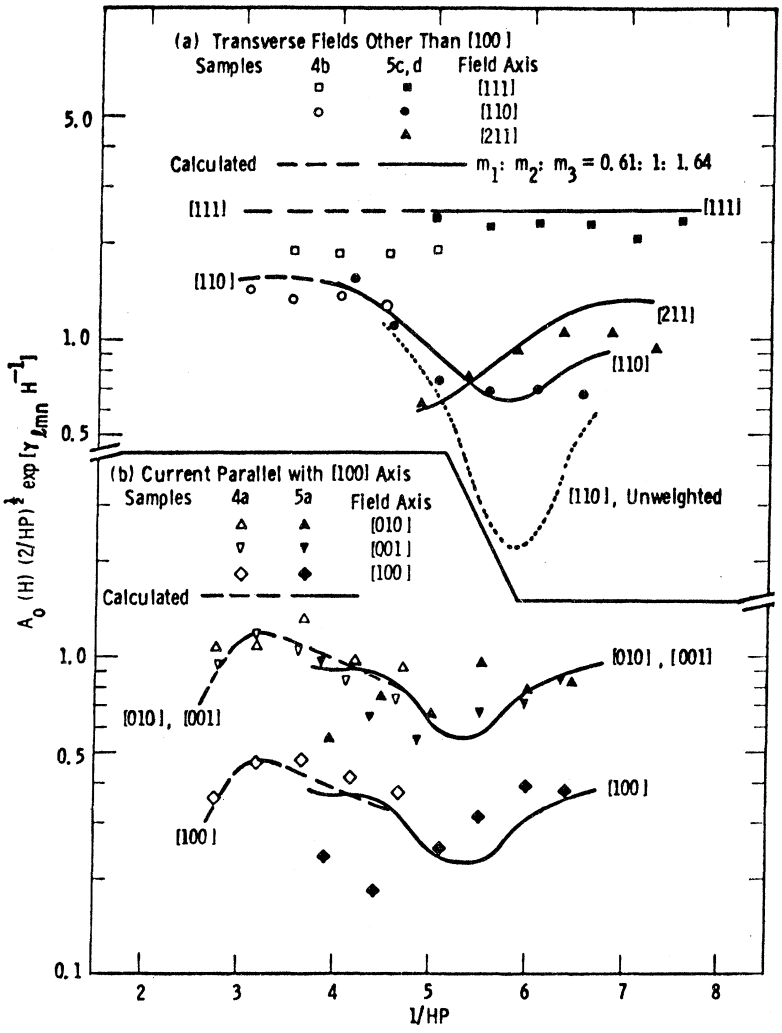

FIG. 8. Zero-temperature amplitudes $A_0(H)$ divided by the expected field dependence of the principal component, $(\frac{1}{2}HP)^{1/2} \times e^{-\gamma/H}$, plotted against $1/HP$. Calculated amplitudes make approximate allowance for interference by more strongly damped components of higher frequency.

The calculated [110] amplitude is exceptional. It will be seen from Table IV that the two lowest areas are nearly equal when H is in a [110] direction, so their dampings are not very different and pronounced beats can appear in the envelope. One such beat occurs at $1/HP = 6.3$; the resulting minimum is shown by the dotted line in Fig. 8, and is shifted from its expected position through the action of a third frequency of lesser amplitude. Such phenomena are sensitive to the weightings of the component frequencies. The full [110] envelope shown in Fig. 8 was obtained by weighting the component due to each band according to the low-field conductivity of that band in the direction of the current. This procedure should not be grossly in error, but is clearly not well justified in a transverse measurement with Hall angle near 45°.

Results from sample 5a—bottom right of Fig. 8—have been ignored in finding the ratio of masses that will fit the amplitudes. The current in this sample is in the [100] direction. The transverse magnetoresistances $H \parallel [010]$ and $H \parallel [001]$ can differ, since the crystal is of class T_h rather than O_h; an estimate of this difference is given by assigning the component amplitudes from each band a magnitude proportional to the conductivity of the band in the direction of the current. It is then found that the two transverse amplitudes do not differ by more than 20%, and that the ratio of longitudinal to mean-transverse amplitude should be very nearly constant. These rules are obeyed by sample 4a, of lower carrier concentration, but not by 5a, as Fig. 8 makes plain. Moreover, for a given value of HP the amplitude obtained from 5a should be close to that obtained from 4a (cf. the [111] and [110] results), but is not. Though results obtained on 5a have been ignored, we must note that the longitudinal amplitudes obtained from it were confirmed by 5b, a similar sample cut from the same part of the ingot as 5a but along another [100] axis.

The value of $\gamma_{[100]}$ is 1.7×10^5 G for both of samples 4b and 5c. We relate this to the mean momen-

tum relaxation time for conduction τ_c: In a spherical band one has

$$\gamma = \pi H/\omega_H \tau_s = (\pi/R\sigma)(\tau_c/\tau_s) .$$

Calculation is only a little more complicated when allowing for ellipsoids; the numerical result for the two samples is $\tau_s/\tau_c = 0.69$ for sample 4b, and $\tau_s/\tau_c = 0.76$ for sample 5c. This is close to the equality of τ_s and τ_c that is expected in the case of completely isotropic scattering; it is usual that τ_s be at least somewhat smaller than τ_c.

4. *Correction to Effective Masses*

The cyclotron masses in Table III are listed together with corrected values obtained through taking account of interference effects. The procedure followed in making the correction is straightforward. From Eq. (4) for the amplitudes we note that at low temperatures $A(H, T) \sim (1 - \lambda m^2 T^2)$, λ being a constant for fixed magnetic field. For, say, two components of magnitudes B_1, B_2 at a particular field, and effective masses m_1 and m_2, the temperature dependence of the total magnetoresistance at low temperatures and fixed magnetic field is approximately

$$\Delta\rho \sim B_1(1 - \lambda m_1^2 T^2) + B_2(1 - \lambda m_2^2 T^2)$$

$$= (B_1 + B_2)(1 - \lambda m_{\text{app}}^2 T^2) ,$$

$$m_{\text{app}}^2 = (B_1 m_1^2 + B_2 m_2^2)/(B_1 + B_2) . \qquad (8)$$

Here m_{app} is the apparent mass that is derived from the temperature dependence. Note that the amplitudes B_1 and B_2 are the values of the oscillatory magnetoresistance at the field in question, not the envelope functions; i.e.,

$$B_i = A_{0i}(H) \cos(2\pi/P_i H - \tfrac{1}{4}\pi) ,$$

not $A_{0i}(H)$. The ratios m_2/m_1 and B_2/B_1 can be obtained from the calculated areas in Table IV and the damping constants γ of Sec. III B 3; this must be done for each field at which the apparent mass was found, and m_{app} corrected to give the value of m_1.

IV. CONCLUSIONS

The valence-band maxima in $PtSb_2$ are six ellipsoids centered on the $\langle 100 \rangle$ axes. The principal inertial effective masses m_1, m_2, and m_3 are unequal, being in the ratio 0.61:1:1.64; at low temperatures the momentum relaxation time is almost isotropic, the quantities m_i/τ_i being in the ratio 0.7:1:1.6. The least cyclotron mass $(m_1 m_2)^{1/2}$ is $(0.168 \pm 0.005)m$, and the density-of-states effective mass per band, $(m_1 m_2 m_3)^{1/3}$, is $0.22m$.

In a search for band interactions, effective masses and areas have been investigated over a range of carrier concentrations corresponding to Fermi levels from 0.004 to 0.015 eV, and no dependence of mass or shape on energy has been detected. The strongly energy-dependent bands suggested by one of us (P. R. E.)[6] are definitely not present. Most models of band interaction give an effective mass that increases with increase in Fermi energy; the results in Table III suggest, if anything, that the mass decreases at greater carrier concentrations. We can certainly exclude any increase greater than 5% over the range of energies measured. A simplified version of Kanes's[14] model of band interactions (which is not strictly appropriate for bands not at $\vec{k} = 0$) gives for the energy dependence of the cyclotron mass $m(E) = m(0)(1 + 2E/E_G)^{-1}$, E_G being the direct band gap. Since m changes by less than 5% when E increases by 0.011 eV, we see that $E_G > 0.4$ eV. One must conclude that the small magnitude of the observed indirect band gap, 0.10 eV, is accidental; the valence and conduction bands do not interact strongly with each other.

ACKNOWLEDGMENTS

We are much indebted to Miss B. J. Kagle for writing the computer programmes that have been used in this work, and to P. Piotrowski and to G. J. Faychak for their assistance in the experiments.

*Present address: Department of Physics, University of Connecticut, Storrs, Connecticut 06268.

[1] R. C. Miller, D. H. Damon, and A. Sagar, J. Appl. Phys. 35, 3582 (1964).

[2] D. H. Damon, R. C. Miller, and A. Sagar, Phys. Rev. 138, A636 (1965).

[3] R. A. Reynolds, M. J. Brau, and R. A. Chapman, J. Phys. Chem. Solids 29, 755 (1968).

[4] C. T. Elliot and S. E. R. Hescocks, J. Natural Sci. 3, 174 (1968).

[5] J. O'Shaughnessy and C. Smith, Solid State Commun. 8, 481 (1970).

[6] P. R. Emtage, Phys. Rev. 138, A246 (1965).

[7] H. Roth, W. D. Straub, W. Bernard, and J. E. Mulhorn, Jr., Phys. Rev. Letters 11, 328 (1963).

[8] L. P. Kao and E. Katz, J. Phys. Chem. Solids 6, 223 (1958).

[9] G. L. Pearson and H. Suhl, Phys. Rev. 83, 768 (1951).

[10] D. H. Damon, Westinghouse Research Report No. 67-1F4-TPROP-R1 (unpublished).

[11] C. Herring and E. Vogt, Phys. Rev. 101, 944 (1956).

[12] L. M. Roth and P. N. Argyres, in *Semiconductors and Semimetals*, edited by R. K. Willardson and A. C. Beer (Academic, New York, 1966), Vol. I, p. 159 ff.

[13] For example, in InAs, which has a spherical band at the zone center [R. J. Sladek, Phys. Rev. 110, 817 (1958)].

[14] E. O. Kane, J. Phys. Chem. Solids 1, 249 (1957).